Sand Detachment with Shallow Asymmetric Corona Formation under Well-Developed Lateral Jets of Wind-Driven Raindrop Impacts

G. Erpul[1], D. Gabriels[2], Ç. Sagun[3], M.Ö. Pınar[4], W. Cornelis[5]

During the last two decades, there has been a significant increase in Wind-Driven Rain (WDR) erosion studies, and it is now well known that soil detachment and sediment transport processes differ under WDR conditions compared to those under Wind-Free Rain (WFR). Raindrop motion using the straight-line physics of WFR cannot elucidate that using the vector physics of WDR (Erpul et al., 2013a, 2013b). Accordingly, sub-processes associated with on-impact (splash corona formation or splash detachment) and after-impact (splash transport) of the WDR erosion also change substantially. On one hand, depending upon the decreases in the compressive stress as lateral jets are well developed, a deep symmetric corona formation becomes much more limited while a shallow asymmetric corona prevails (Erpul et al., 2002). On the other hand, the WDR splash trajectory becomes almost unidirectional in the prevailing wind direction unlike the radial sand splashes of WFR (Erpul et al., 2005).

In this research, the effects of WDR on sand detachment were studied under various obliquities - different magnitudes of raindrop compressive and lateral stresses - with a two dimensional experimental set-up in the wind tunnel facility of the International Center for Eremology (ICE), Ghent University, Belgium (Gabriels et al., 1997; Cornelis et al., 2004). During the experiments, sand particles in splash cups were exposed to both WFR and WDR driven by horizontal wind velocities of 6.4, 8.9 and 12.8 m s^{-1} under rainfall intensities of 50, 60, 75 and 90 mm h^{-1} to assess sand detachment rate (D, g $m^{-2}s^{-1}$). Together with the varied WDR intensities and fall trajectories of synchronized wind and rain simulations, two different sand sizes (2.0 mm & 0.2-0.5 mm) and sand moisture conditions (dry & wet) were also used. The partition of normal and horizontal kinetic energy fluxes (KE_x and KE_y, respectively) is graphed in Figure 1, which clearly shows that the experiments were performed under increasing lateral jets of wind-driven raindrops as their compressive normal components remained almost unchanged for WDR with wind of 6.4, 8.9 and 12.8 m s^{-1} velocities.

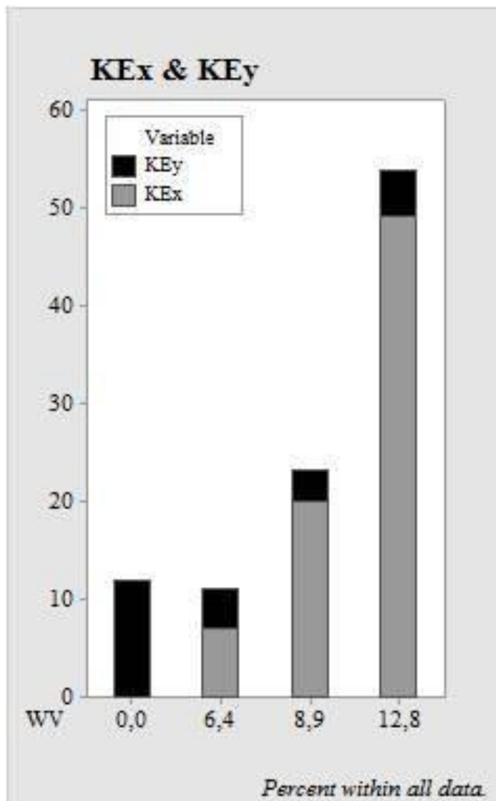

Figure 1. Vertical and horizontal kinetic energy partitioning (KEx & KEy).

[1]Gunay Erpul, Professor, Faculty of Agr., Dept. of Soil Sci. and Plant Nutrition, Ankara University, Ankara, Turkey; [2]Donald Gabriels, UNESCO Chair on Eremology, Dept. of Soil Mgmt., Ghent University, Ghent, Belgium; [3]Caglar Sagun, Ph.D. candidate, Graduate School of Natural and Applied Sci., Dept. of Soil Sci. and Plant Nutrition, Ankara University, Ankara, Turkey; [4]Melis Ö. Pinar, Ph.D. candidate, Graduate School of Natural and Applied Sci., Dept. of Soil Sci. and Plant Nutrition, Ankara University, Ankara, Turkey, and MoFAL – Transitional Zone Agricultural Research Institute, Eskisehir, Turkey; [5]Wim Cornelius, Dept. of Soil Mgmt. and Soil Care, Ghent University, Ghent, Belgium. Corresponding author: M.Ö. Pinar, email: melisozge.pinar@gthb.gov.tr.

Table 1. Measured sand detachment rates (0.2-0.5 mm dry/wet and 2.00 mm dry & wet) under the research simulated rainfall intensities (50, 60, 75 and 90 mm h^{-1}) of WFR and WDR using the reference wind velocities of 6.4, 8.9, and 12.8 m s^{-1}.

WV, u (m s^{-1})	Median drop size, d_{50} (mm)	Rainfall obliquity			I, Rain intensity (mm h^{-1})	Kinetic energy partition (J m^{-2} s^{-1})			Sand detachment rate (D, g/$m^{-2}s^{-1}$)			
		Rain inclination α (degree)	Cos α (degree)	Sin α (degree)		KE_x	KE_y	KE_r	D_{dry} [0.2-0.5 mm]	D_{wet} [0.2-0.5 mm]	D_{dry} [2.00 mm]	D_{wet} [2.00 mm]
0	1	0	1	0	50	0	0.159	0.159	0.10±0.02*	0.16±0.03	0.28±0.02	0.08±0.02
					60	0	0.191	0.191	0.16±0.11	0.26±0.22	0.25±0.15	0.15±0.10
					75	0	0.239	0.239	0.32±0.15	0.35±0.20	0.31±0.07	0.16±0.05
					90	0	0.286	0.286	0.36±0.19	0.36±0.11	0.46±0.27	0.42±0.44
6.4	1.63	53	0.60	0.80	50	0.095	0.101	0.195	0.41±0.09	0.56±0.03	0.71±0.18	0.59±0.02
					60	0.114	0.121	0.234	0.59±0.16	0.68±0.12	1.00±0.23	0.66±0.15
					75	0.142	0.151	0.293	0.80±0.25	0.98±0.23	1.02±0.13	1.08±0.14
					90	0.170	0.181	0.352	0.88±0.09	1.01±0.17	1.19±0.12	1.11±0.05
8.9	1.53	68	0.37	0.93	50	0.266	0.268	0.535	1.20±0.03	1.39±0.28	1.09±0.04	1.25±0.16
					60	0.320	0.322	0.641	1.30±0.21	1.76±0.09	1.99±0.02	1.63±0.03
					75	0.399	0.402	0.802	1.75±0.42	2.18±0.09	2.44±0.14	2.03±0.04
					90	0.479	0.483	0.962	1.88±0.18	2.26±0.09	2.80±0.53	2.18±0.13
12.8	1.54	73	0.28	0.96	50	0.657	0.659	1.317	2.83±0.47	2.90±0.37	2.88±0.20	2.56±0.31
					60	0.789	0.791	1.580	3.19±0.23	3.26±0.22	2.88±0.51	2.98±0.09
					75	0.986	0.988	1.975	3.58±0.58	3.93±0.36	3.63±0.06	3.48±0.001
					90	1.183	1.186	2.370	3.71±0.33	3.95±0.09	3.94±0.03	3.82±0.10

*Mean values are provided along with standard deviations. WV-wind velocity; KE_x-horizontal kinetic energy flux; KE_y-vertical kinetic energy flux; KE_r-resultant kinetic energy flux; D-sand detachment rate.

The measured sand detachment rates (0.2-0.5 mm dry/wet and 2.00 mm dry/wet) are reported in Table 1 as mean values along with standard deviations indicated by the ± sign. The factorial ANOVA showed that the two components of the kinetic energy flux term (KE_x and KE_y, J m^{-2} s^{-1}), which integrate the frequency, angle and velocity of WDR, explained the variation in D (P<0.05), and neither sand size nor moisture content was statistically significant alone, although binary interactions of KE_x and KE_y with sand size were significant. The vertical kinetic energy flux term (KE_y, $Jm^{-2}s^{-1}$) was statistically significant in windless rain conditions, for which the vertical kinetic energy flux was equal to the resultant kinetic energy flux ($KE_y = KE_r$). Additionally, the correlation matrix (Table 2) underpinned the greater significance of tangential stresses in sand detachment when compared to compressive stresses in the improved lateral jets of WDR conditions.

Table 2. Pearson correlation coefficients between the sand detachment rates (0.2-0.5 mm dry/wet & 2.00 mm dry/wet) and the vectorial kinetic energy fluxes (KE_X. KE_Y & KE_r, J $m^{-2}s^{-1}$) under WDR.

	KE_r	KE_x	KE_y
$D_{dry[0.2-0.5]}$ ($g/m^{-2}s^{-1}$)	0.958	0.961	0.492
	0.000	0.000	0.002
$D_{wet[0.2-0.5]}$ ($g/m^{-2}s^{-1}$)	0.967	0.971	0.491
	0.000	0.000	0.002
$D_{dry[2.00]}$ ($g/m^{-2}s^{-1}$)	0.935	0.936	0.520
	0.000	0.000	0.001
$D_{wet[2.00]}$ ($g/m^{-2}s^{-1}$)	0.980	0.981	0.551
	0.000	0.000	0.000

Experimental data with splash cups directly taken on sand detachment with shallow asymmetric corona formation have been provided in this study, to allow for better insight into the process under the well-developed lateral jets of wind-driven raindrop impacts.

References

Cornelis, W., G. Erpul, and D. Gabriels. 2004. The I.C.E. wind tunnel for wind and water interaction research. In wind and rain interaction in erosion, S. Visser and W. Cornelis (eds.), Tropical Resource Management Papers, Chapter 13. Wageningen University and Research Centre: Wageningen, The Netherlands. pp. 195-224.

Erpul, G., D. Gabriels, L.D. Norton, D.C. Flanagan, C. Huang, and S. Visser. 2013a. Mechanics of interrill erosion with wind-driven rain. Earth Surf. Proc. Landforms 38: 160–168.

Erpul, G., D. Gabriels, L.D. Norton, D.C. Flanagan, C. Huang, and S. Visser. 2013b. Raindrop and flow interactions for interrill erosion with wind-driven rain. J. Hydraul. Res. 51(5): 548-557.

Erpul, G., D. Gabriels, and L.D. Norton. 2005. Sand detachment by wind-driven raindrops. Earth Surf. Proc. Landforms 30: 241-250.

Erpul, G., L.D. Norton, and D. Gabriels. 2002. The effect of wind on raindrop impact and rainsplash detachment. Trans. ASAE 46(1): 51-62.

Gabriels, D., W. Cornelis, I. Pollet, T. Van Coillie, and M. Quessar. 1997. The I.C.E. wind tunnel for wind and water erosion studies. Soil Tech. 10: 1-8.